A Combined Approach for Detection and Deconvolution

Technical Report

J-L. Starck

DSM/DAPNIA/SEI-SAP, CEA/Saclay, 91191 Gif-sur-Yvette, France

January 1999 - Version 1.0

1 Introduction

Astronomical images contain typically a large set of point-like sources (the stars), some quasi point-like objects (faint galaxies, double stars) and some complex and diffuse structures (galaxies, nebulae, planetary stars, clusters, etc.). These objects are often hierarchically organized: star in a small nebula, itself embedded in a galaxy arm, itself included in a galaxy, and so on.

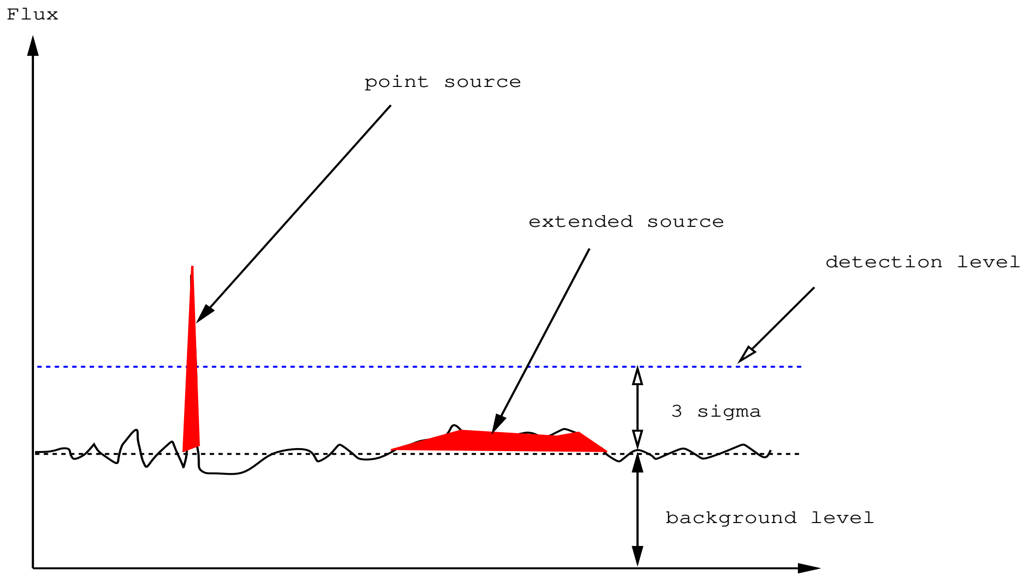

Figure 1: Example of astronomical data: a ponctual and an extended source are shown, with noise and background. The extended object, which can be detected by eyes is undetected by a standard approach.

A standard approach to source detection consists in the four following steps:

- Background estimation
- Noise etimation
- Detection where flux > Background + k * Noise
- Gaussian or PSF (for point source) fitting to derive the photometry

Faint extended objects may be lost by this standard approach. Figure 1 shows a typical example where a faint extended object is under the detection limit. In order to detect faint objects, whatever their sizes, Bijaoui and Rué [1] have proposed the Multiscale Vision Model (MVM).

A *vision model* is defined as the sequence of operations required for automated image analysis. Taking into account the scientific purposes, the characteristics of the objects and the existence of hierarchical structures, astronomical images need specific vision models. This is also the case in many other fields, such as remote sensing, hydrodynamic flows or biological studies. Specific vision models have been implemented for these kind of images.

We first introduce the MVM as defined in [1], then we present how a deconvolution can be combined to objects reconstruction, and shows that such an approach improves the photometry of the reconstructed objects and helps for an object identification.

2 Multiscale vision model

2.1 Introduction

After applying the wavelet transform on the image, we have to detect, to extract, to measure and to recognize the significant structures. The wavelet space of a 2D direct space is a 3D one. An object has to be defined in this space. A general idea for object definition lies in the connectivity property. An object occupies a physical region, and in this region we can join any pixel to other ones. The connectivity in the direct space has to be transported to the wavelet transform space (WTS). In order to define the objects we have to identify the WTS pixels we can attribute to the objects.

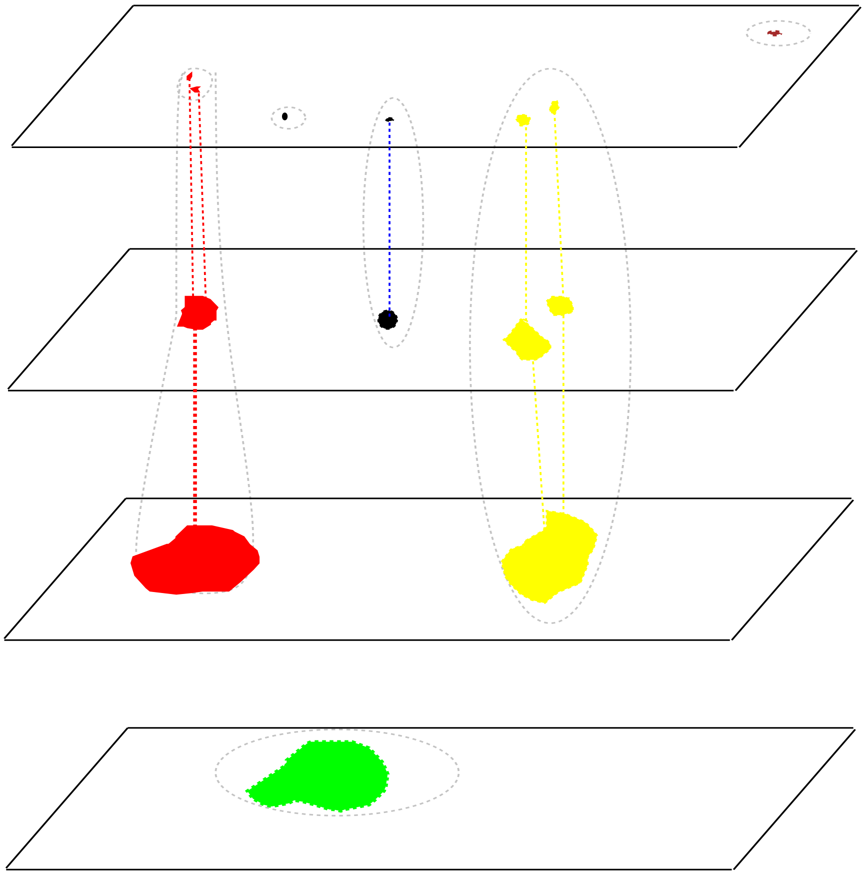

Figure 2: Example of connectivity in the wavelet space: contiguous significant wavelet coefficients form a structure, and following an interscale relation, a set of structures form an object. Two structures S_j, S_{j+1} at two successive scales belongs to the same object if the position pixel of the maximum wavelet coefficient value of S_j is included in S_{j+1}.

Figure 2.1 shows an example of connectivity between detected structures at different scales.

2.2 Definition

The Multiscale Vision Model (MVM) [1, 5] described an object as a hierarchical set of structures. It uses the following definitions:

- Significant wavelet coefficient: a wavelet coefficient is significant when its absolute value is upper a given detection limit. The detection limit depends on the noise modeling (Gaussian noise, Poisson noise, ...). See [7] for a full desription of the noise modeling.
- **Structure**: a structure $\mathcal{S}_j$ is a set of significant connected wavelet coefficients at the same scale j.
- **object**: an object is a set of structures.
- **object scale**: the scale of an object is given by the scale of the maximum of its wavelet coefficients.
- **interscale-relation**: the law will allows us to connect two structures into a single object is called "interscale-relation". Let us consider two structures at two successive scales, S_j^1 and S_{j+1}^2. Each structure is located on one of the individual images of the decomposition and corresponds to a region in this image where the signal is significant. Noting p_m the pixel position of the maximum wavelet coefficient value of S_j^1, S_j^1 is said to be connected to S_{j+1}^2 if S_{j+1}^2 contains the pixel position p_m (i.e. the maximum position of the structure S_j^1 must also be contained in the structure S_{j+1}^2). Several structures appearing on successive wavelet coefficient images can be connected in such a way, which we call an object in the interscale connectivity graph.
- **sub-object**: a sub-object is a part of an object. It appears when an object has a local wavelet maximum. Hence, an object can be composed of several sub-objects. Each sub-object can also be analysed.

2.3 Reconstruction

The problem of reconstruction [1, 5] consists in searching a signal O such that its wavelet coefficients are the same than those of the detected structures. If $\mathcal{T}$ describes the wavelet transform operator, and P_w the projection operator in the subspace of the detected coefficients (i.e. set to zero all coefficients at scales and positions where nothing where detected), the solution is found by minimization of

$$J(O) = \parallel W - (P_w \circ \mathcal{T})O \parallel$$

where W represents the detected wavelet coefficients of the data. More details can be found in [1].

2.4 Examples

Band extraction in 1D signal

A simulated spectrum has been created containing a smooth continuum with superimposed, variable Gaussian noise and anemission band at 3.50μm with a maximum of five times the local noise standard deviation and a width of FWHM $= 0.01\mu$m (see Figure 3 top). Figure 3 (middle) shows the comparison of the reconstructed emission band with the original Gaussian. Figure 3 (bottom) shows the difference between the simulated spectrum and the reconstructed band.

Stars subtraction in NGC2997

Figure 4 shows how stars and HII regions of a galaxy can extracted from an image using the MVM. All object, detected in the two first scales are subtracted from the input image.

2.5 Remarks

The MVM presents many advantages compared to the standard approach

- faint extended objects can be detected as well as point sources.
- the analysis does not require a background estimation.
- the Point Spread Function (PSF) is not needed.

The second point is relatively important. Indeed, if the background varies spatially, its estimation becomes a non-trivial task, and may produce large errors in the object photometry.

The last point is an advantage when the PSF is unknown, or difficult to estimate, which appends relatively often when it is space variant. However, when the PSF is well determined, it becomes a drawback because a know information is not used for the object reconstruction. It leads to systematic errors in the photometry, which depends on PSF and on the source signal to noise ratio. In order to correct this error, a kind of calibration must be performed using simulations [6]. Next section shows how the PSF can be used in the MVM, leading to a deconvolution.

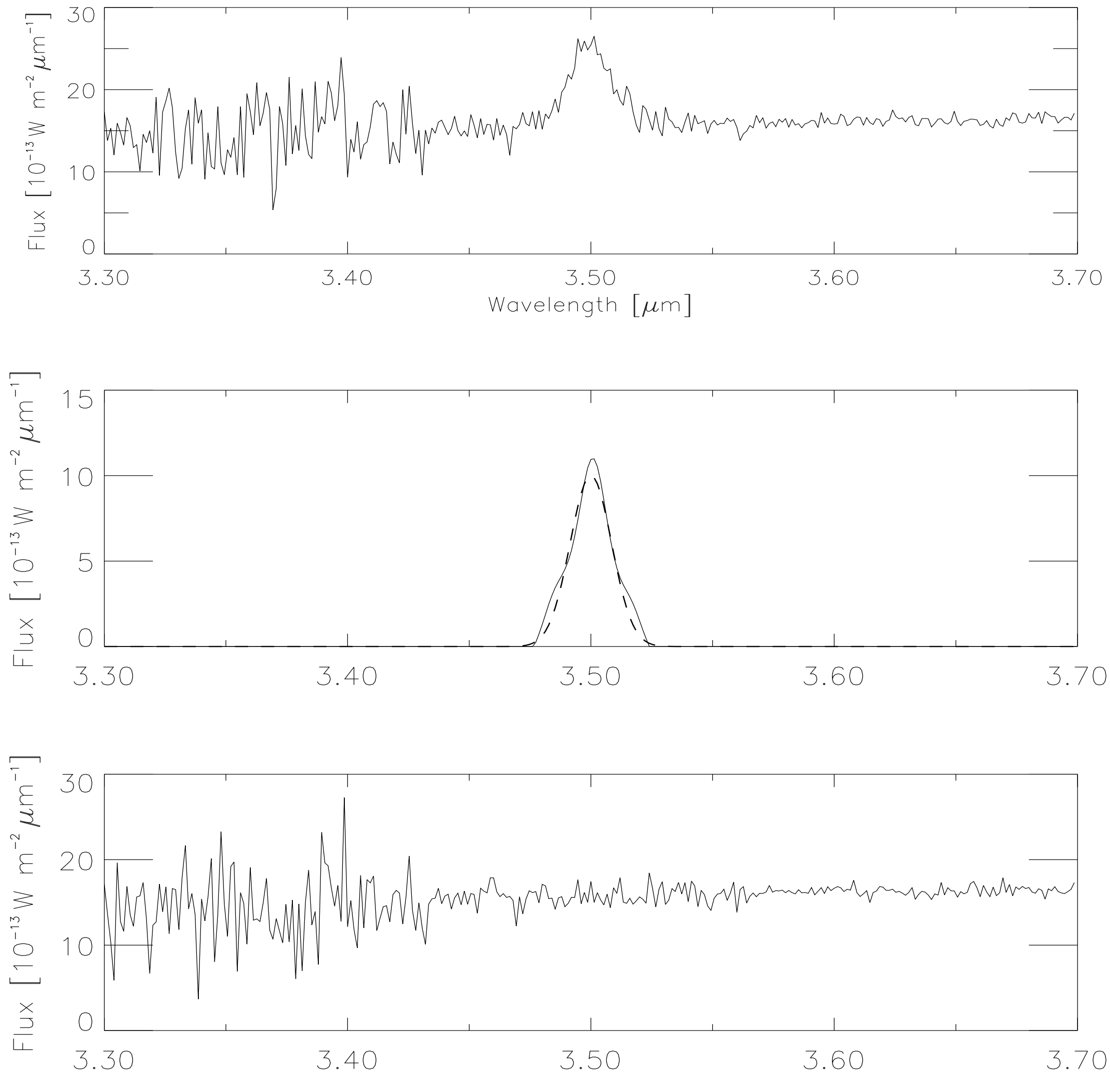

Figure 3: Simulation: top, simulated spectrum, middle, reconstructed simulated band (full line) and original band (dashed line). Bottom, simulated spectrum minus the reconstructed band.

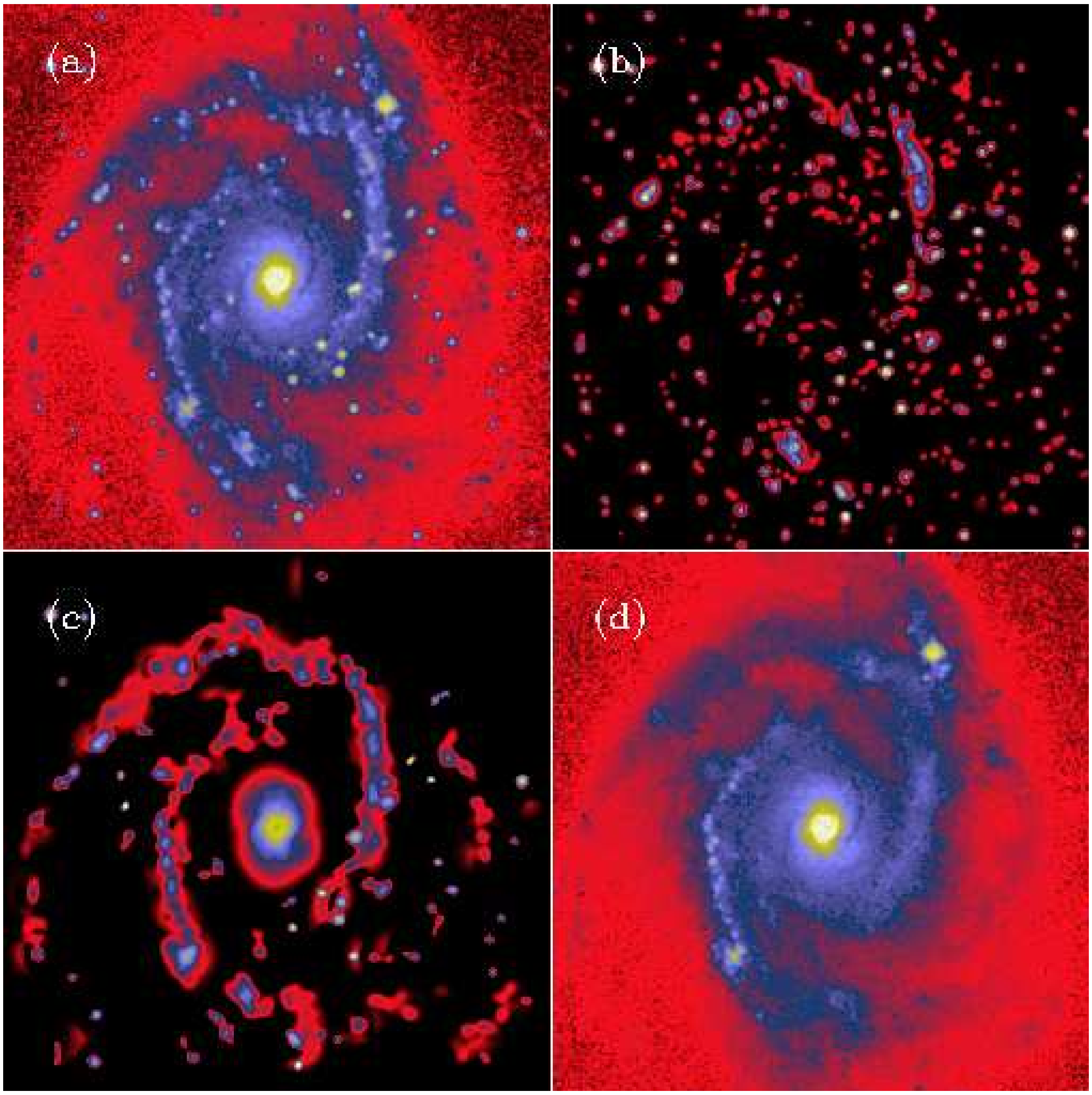

Figure 4: (a) Galaxy NGC2997, (b) objects detected from scale 1 to 2, (c) objects detected from scale 3 to 6, and (d) difference between (a) and (b).

3 Detection and Deconvolution

3.1 The deconvolution problem

Consider an image characterized by its intensity distribution (the "data") $I(x,y)$, corresponding to the observation of a "real image" $O(x,y)$ through an optical system. If the imaging system is linear and shift-invariant, the relation between the object and the image in the same coordinate frame is a convolution:

$$I(x,y) = (O * P)(x,y) + N(x,y) \tag{1}$$

$P(x,y)$ is the point spread function (PSF) of the imaging system, and $N(x,y)$ is an additive noise. In practice $O * P$ is subject to non-stationary noise. We want to determine $O(x,y)$ knowing $I(x,y)$ and $P(x,y)$. This inverse problem has led to a large amount of work, the main difficulties being the existence of: (i) a cut-off frequency of the PSF, and (ii) the noise.

Eq. 1 is always an ill-posed problem. This means that there is not a unique least-squares solution of minimal norm $\| I(x,y) - P(x,y) * O(x,y) \|$, and some constraints must be added in order to regularize the problem [2, 4, 7]. Once the deconvolved image is obtained, it is generally difficult to know what is the noise level in the deconvolved image, and hence, it becomes to detected the objects with a confidence interval. For this reasons, astronomers generally prefer to apply the detection on non-deconvolved images. Another reason against deconvolution is that is has been showns that some regularization methods like MEM [3] affects the photometry.

3.2 Object reconstruction using the PSF

A reconstructed and deconvolved object can be obtained by searching a signal O such that the wavelet coefficients of $P * O$ are the same than those of the detected structures. If $\mathcal{T}$ describes the wavelet transform operator, and P_w the projection operator in the subspace of the detected coefficients, the solution is found by minimization of

$$J(O) = \| W - (P_w \circ \mathcal{T}) P * O \| \tag{2}$$

where W represents the detected wavelet coefficients of the data, and P is the point spread function. By this approach, each object is deconvolved separately. The flux related to the ring of the PSF will be taken into account. For point source, the solution will be close to those obtained by PSF fitting. This problem is also different from the global deconvolution in the sense that it is well constraint. Exept the positivity of the solution which is always true and must be used, no other constraint need to be introduced. This is due to the fact that the reconstruction is performed from a small set of wavelet coefficients (those upper a detection limit). The number of objects are the same than those obtained by the MVM, but the photometry and the morphology is different. The position may also change a little bit.

3.3 The algorithm

Any minimizing method can be used to obtain the solution O. As we did not meet any problem of convergence, noise amplification, or ringing effect, we choose the Van Cittert method, which is certainly the simplest one. For each detected object, we apply the following algorithm:

$$O^{n+1} = O^n + \mathcal{T}^{-1}(W - (P_w \circ \mathcal{T}) P * O^n) \tag{3}$$

where $\mathcal{T}^{-1}$ is the inverse wavelet transform.

1. Set n to 0.
2. Find the initial estimation O^n by applying an inverse wavelet transform to the set W corresponding to the detected wavelet coefficients in the data.
3. Convolve O^n by the PSF P: $I^n = P * O^n$.
4. Determine the wavelet transforn $W(I^n)$ of I^n.
5. Threshold all wavelet coefficients in $W(I^n)$ at position and scales where nothing has been detected (i.e. P_w operator). We get $W_t(I^n)$.
6. Determine the residual $W(R) = W - W_t(I^n)$.
7. Reconstructed the residual image R^n applying an inverse wavelet transform.
8. Add the residual to the solution: $O^{n+1} = O^n + R^n$.
9. Threshold negative values in O^{n+1}.
10. if $\sigma(R^n)/\sigma(O^0) < \epsilon$ then $n = n + 1$ and goto step 3.
11. O^{n+1} contains the deconvolved reconstructed object.

In practice, the convergence is very fast (less than 20 iterations). The reconstructed image (not deconvolved) can also be obtained, just by reconvolving the solution by the PSF.

3.4 Examples

Point source reconstruction

A simulation has been performed in order to analyse how well the flux is estimated. A point source (using ISOCASM 6 arc-second lens PSF) has been simulated, with a constant background (value of 100), and a uniform Gaussian noise (sigma=1). The integrated flux of the source vary from 7 to 102. Table 1 gives the results of this simulation. The first column gives the real flux, the second column the flux found using MVM, and the third column the flux found using MVM plus the devonvolution (MVMD). The photometry is clearly improved using MVMD. Another aspect of MVMD is that the error is relatively constant, whatever the flux of the source.

Figure 5 shows the estimated flux versus the real flux for both MVM (dotted line) and MVMD (dashed line) methods. The full line corresponds to the perfect case (estimated flux = real flux). The better linearity of the MVMD estimated flux can be seen.

Abell 1689 ISOCAM data

Figure 6 shows the detections (isophot) obtained using the MVM method without deconvolution on ISOCAM data. The data were collected using the 6 arc second lens at 6.75μm. It was a raster observation with 10s integration time, 16 raster positions, and 25 frames per raster position. The noise is non stationary, and the detection of the significant wavelet coefficients was done using the root mean square error map $R_\sigma(x, y)$ by the method described in [6]. The isophot are overplotted on a optical image (NTT, bande V) in order to identify the infrared source. Figure 7 shows the same treatment but using the MVM method with deconvolution. The object are the same, but the photometry is improved, and it is clearly easier to identify the optical counterpart of the infrared sources.

Table 1: Flux estimation from MVM and MVM + deconvolution (MVMD).

Real Flux	MVM Flux	MVMD Flux	MVM Error	MVM Error (%)	MVMD Error	MVMD Error (%)
7	7.35	5.96	5.00	14.82	0.35	1.03
12	12.66	12.62	5.51	5.21	0.66	0.62
17	17.57	18.41	3.37	8.30	0.57	1.41
22	21.68	23.42	1.41	6.46	0.31	1.42
27	26.18	28.43	3.00	5.31	0.81	1.43
32	30.74	33.44	3.93	4.51	1.25	1.44
37	35.28	38.45	4.64	3.93	1.71	1.45
42	39.91	43.46	4.95	3.49	2.08	1.46
47	44.60	48.47	5.09	3.13	2.39	1.47
52	49.24	53.48	5.29	2.85	2.75	1.48
57	53.93	58.49	5.37	2.61	3.06	1.49
62	58.67	63.49	5.36	2.41	3.32	1.49
67	63.42	68.50	5.33	2.24	3.57	1.50
72	68.14	73.51	5.35	2.09	3.85	1.51
77	72.93	78.51	5.27	1.96	4.06	1.51
82	77.70	83.52	5.23	1.85	4.29	1.52
87	82.47	88.52	5.20	1.75	4.52	1.52
92	87.24	93.53	5.16	1.66	4.75	1.53
97	92.02	98.53	5.13	1.58	4.97	1.53
102	96.84	103.5	5.05	1.50	5.15	1.53

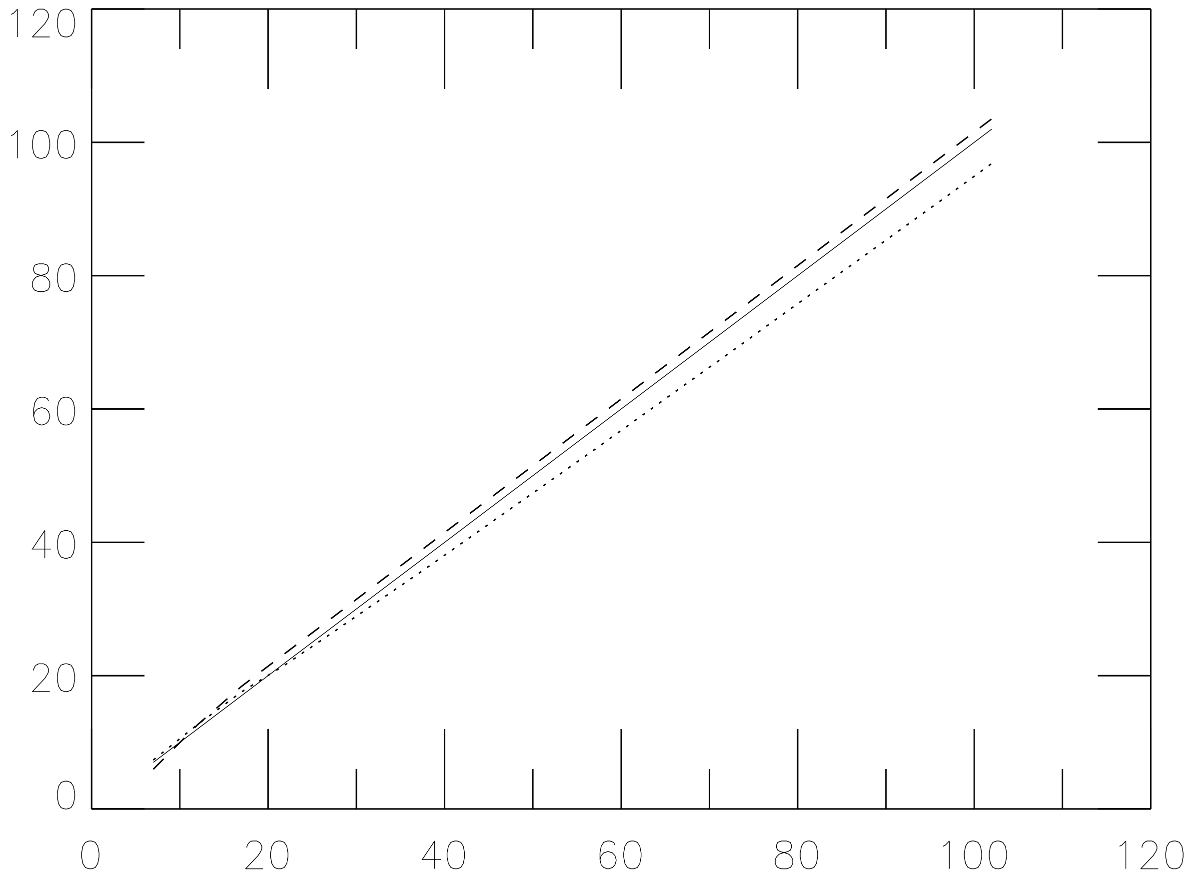

Figure 5: Estimated flux versus the real flux for both MVM (dotted line) and MVMD (dashed line) methods.

References

[1] A. Bijaoui and F. Rué. A multiscale vision model adapted to the astronomical images. *Signal Processing*, 46:229–243, 1995.

[2] R. C. Gonzalez. *Digital Image Processing.* Addison-Wesley Publishing Company, 1993.

[3] R. Narayan and R. Nityananda. Maximum entropy image restoration in astronomy. *Ann. Rev. Astron. Astrophys.*, 24:127–170, 1986.

[4] W.K. Pratt. *Digital Image Processing.* John Wiley & Sons, a wiley-interscience publication edition, 1991.

[5] F. Rué and A. Bijaoui. A multiscale vision model to analyse field astronomical images. *Experimental AStronomy*, 7(3):129–160, 1997.

[6] J.L. Starck, H. Aussel, D. Elbaz, D. Fadda, and C. Cesarsky. Faint source detection in isocam images with preti. *Astronomy and Astrophysics*, 1999. submitted.

[7] J.L. Starck, F. Murtagh, and A. Bijaoui. *Image Processing and Data Analysis: The Multiscale Approach.* Cambridge University Press, Cambridge (GB), 1998.

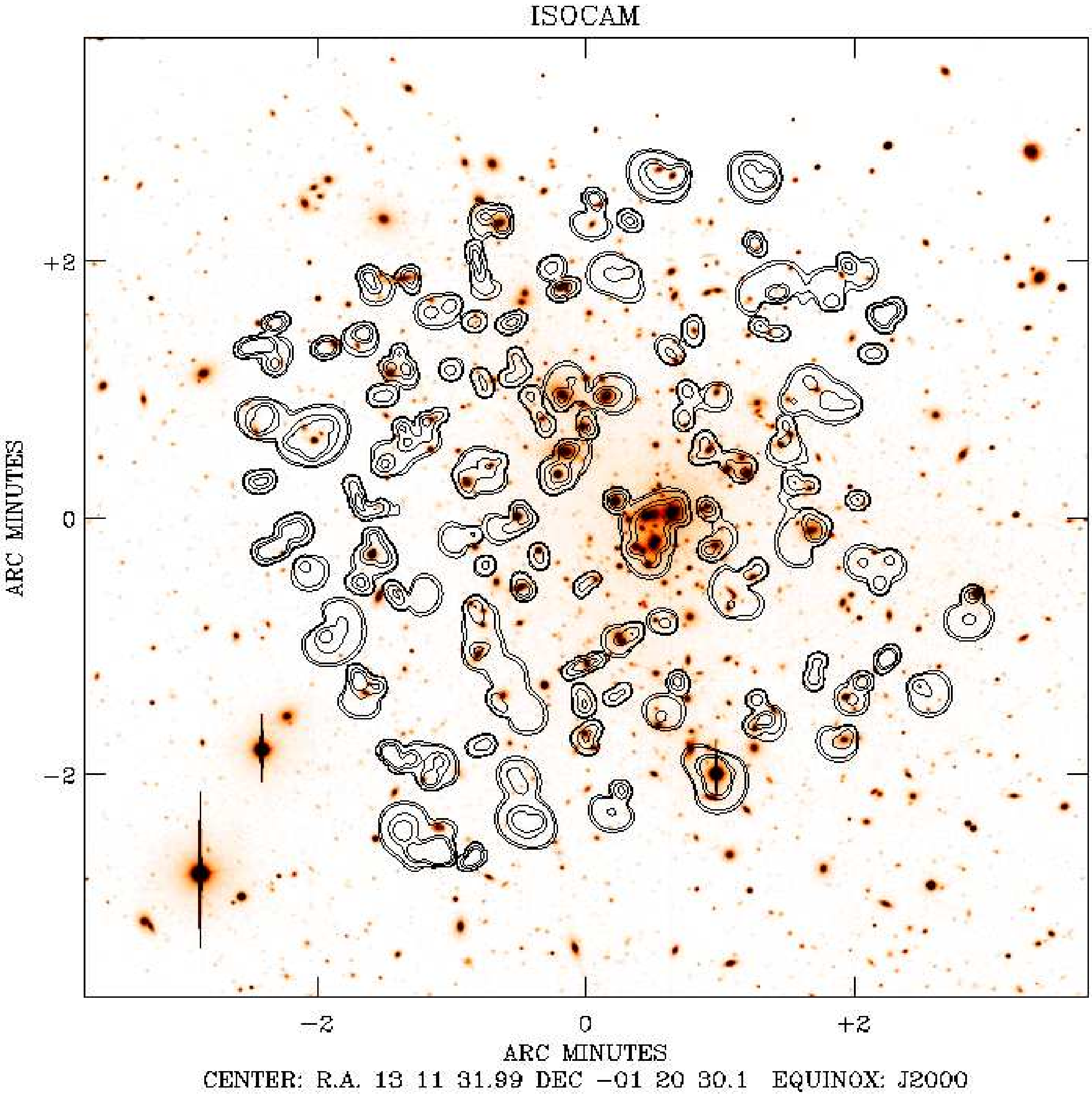

Figure 6: Abell 1689: ISOCAM source detection (isophot) overplotted on an optical image (NTT, bande V). The ISOCAM image is a raster observation at 7 μm.

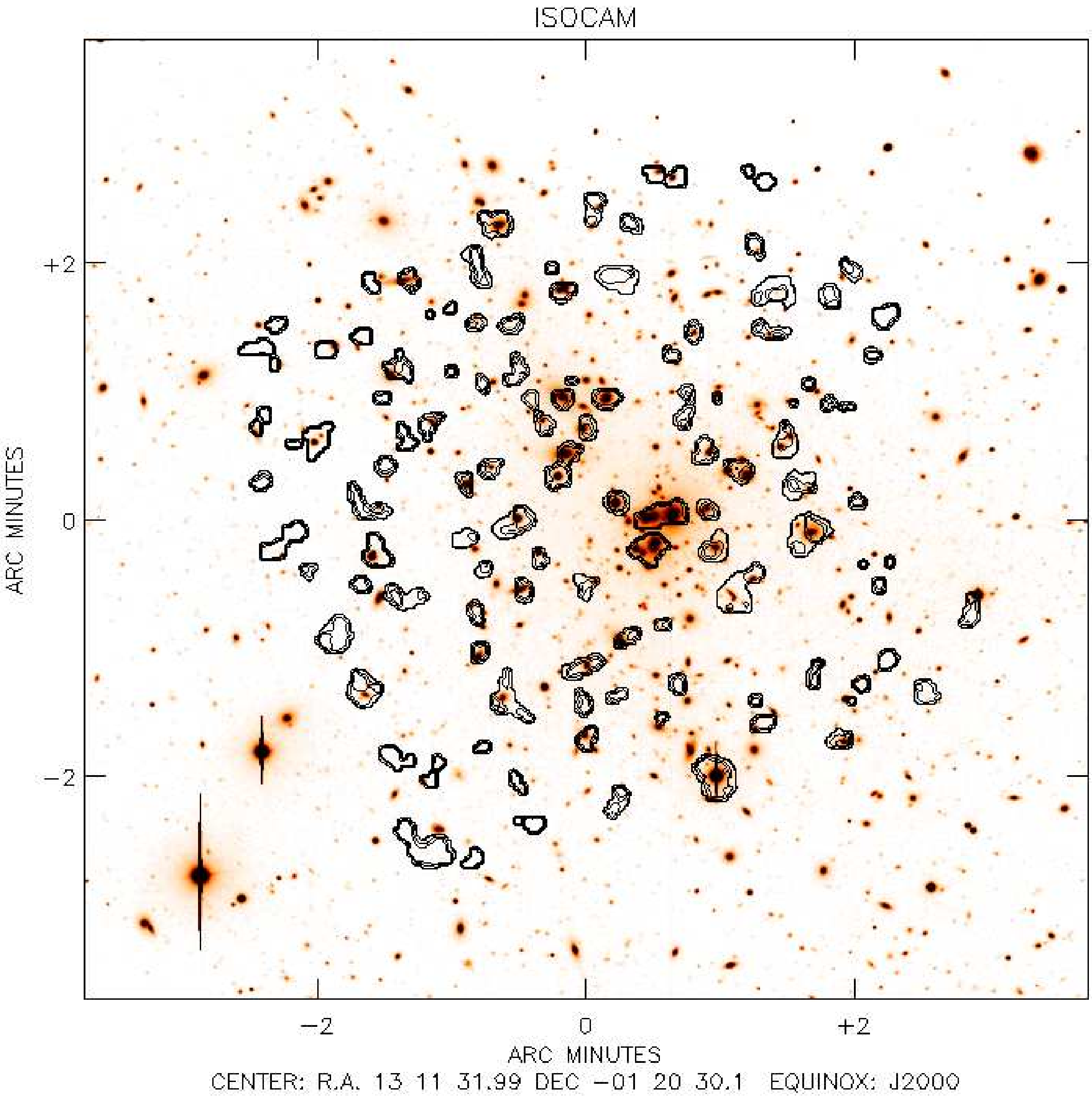

Figure 7: Abell 1689: ISOCAM source detection using the PSF (isophot) overplotted on an optical image (NTT, bande V). Compared to the previous figure, it is clearly easier to identify the detected infrared sources on the optical image.